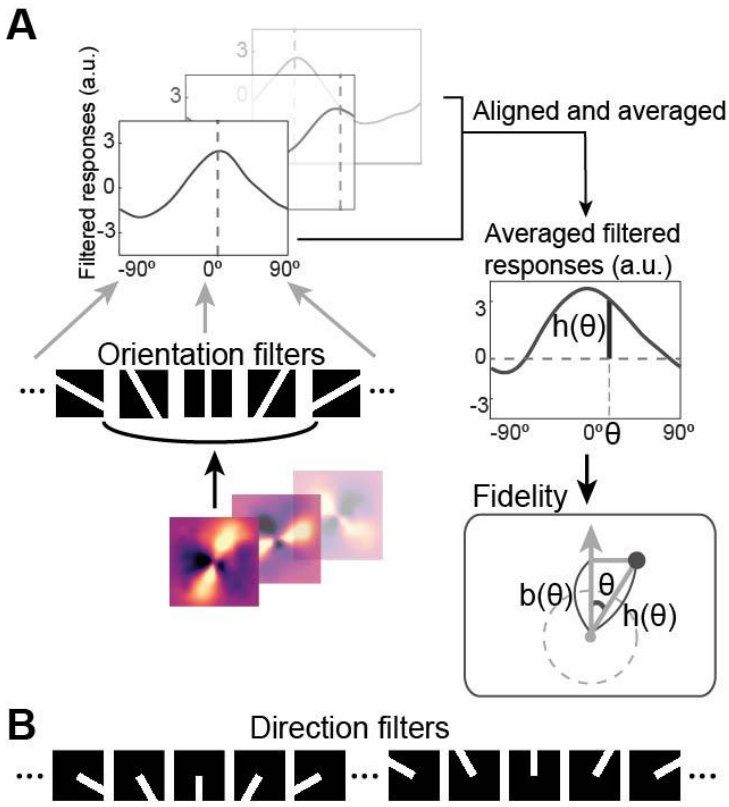

Schematics for computing reconstruction fidelity, related to STAR Methods.

(A) To quantify how well the angle of the stripe in the reconstruction maps matched that of the actual orientation/direction maintained in WM, we built orientation filters which were image masks of line shapes oriented between -90º and 90º in steps of 1º. For each feature condition, filtered responses were computed by multiplying each filter image mask and the reconstruction map image matrix, resulting in a tuning curve-like function. These filtered responses were aligned and averaged across the feature conditions. With the filtered responses, the fidelity metric was computed — whether and how strongly the reconstruction points to the correct direction — by solving for vector $b(\theta)$ for each filter θ using the cosine function ($b(\theta) = h(\theta) \times cos(\theta)$) and taking the average.

(B) Direction filters were used to quantify whether the representation of remembered direction differs in strength between locations in the topographic map corresponding to the terminus and inception of motion direction. Direction filters spanned 360º of polar angle, from -90º to 270º in steps of 1º, where the true orientations of the directions were aligned to be 0º and 180º. The same process was repeated as in (A) for computing the fidelity metric.

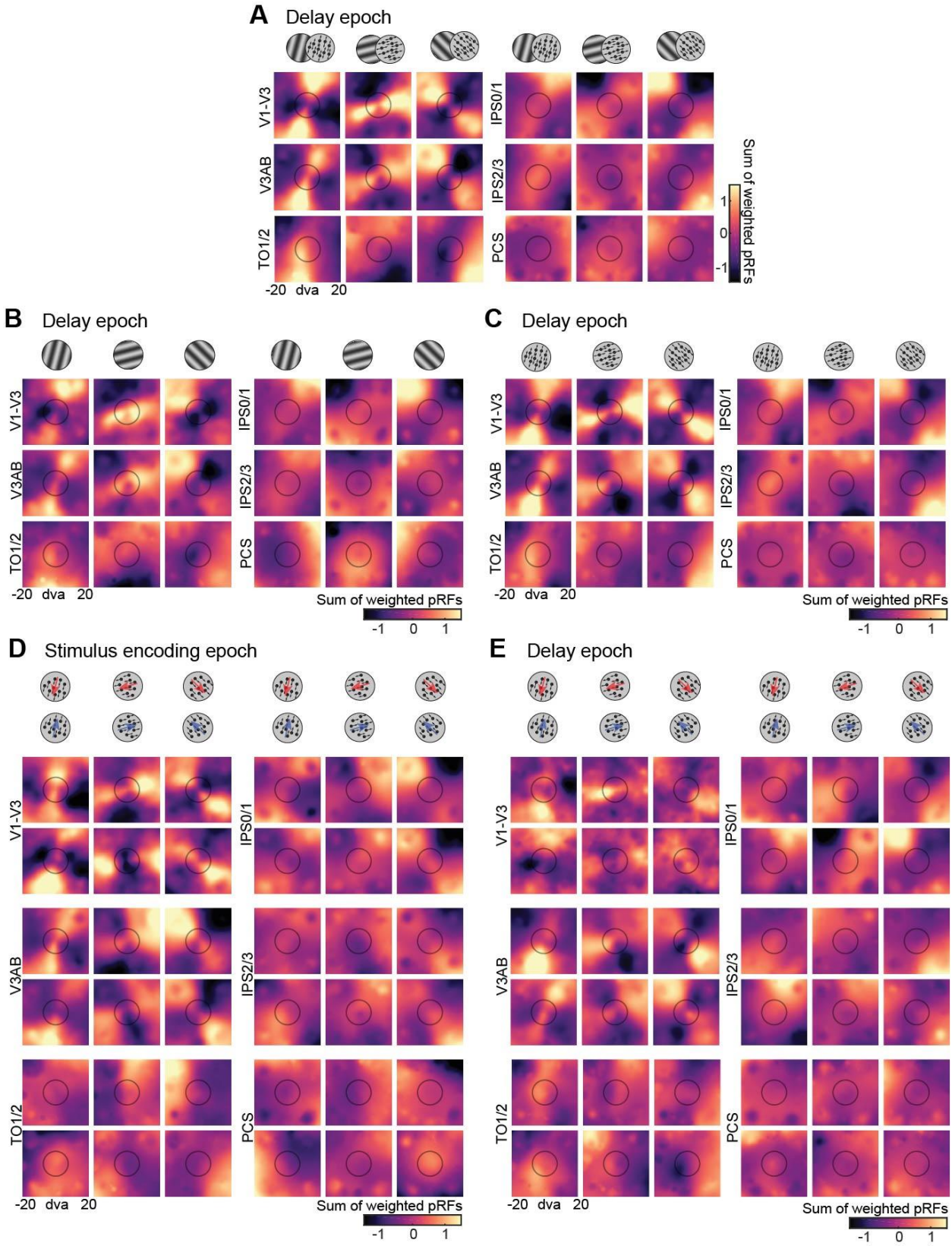

pRF normalized spatial reconstruction maps, related to STAR Methods. We

addressed the possibility that the spatial reconstruction maps are influenced by biases in the pRF structure which differ by individuals. For instance, more voxels in a certain part of the visual field might bias the reconstruction maps, as we are summing up all voxels' pRFs weighted by their beta coefficients. However, even when taking into account the potential bias in pRF structure, results are similar to reconstruction maps without pRF normalization.
(A) Delay epoch, orientation and motion direction trials combined.
(B) Delay epoch, orientation trials.
(C) Delay epoch, motion direction trials (opposite direction conditions sharing the same orientation axis combined).
(D) Stimulus encoding epoch, motion direction trials (separately for each of the 6 direction conditions).
(E) Delay epoch, motion direction trials (separately for each of the 6 direction conditions).
For all figures, the size of each map is from -20° to 20° of visual angle (dva), and the stimulus size is shown for reference in black circles. For (D-E) each of the 6 motion direction schematics on the top correspond to each of the 6 maps for a given ROI.

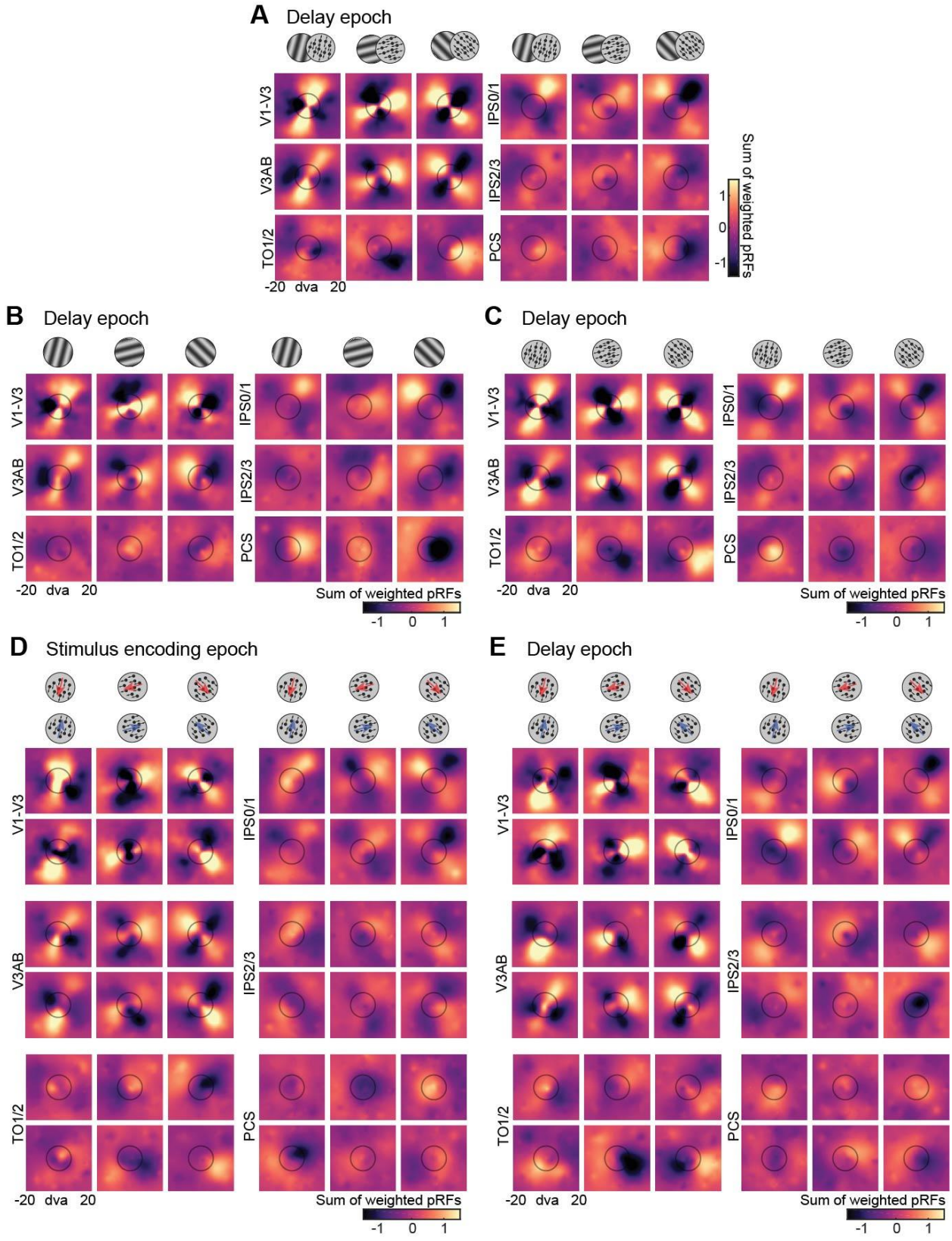

Spatial reconstruction analysis with classifier weights, related to STAR Methods. Weights estimated from the classification algorithm were used for the reconstruction

analysis. We replicated the line format corresponding to the remembered orientation and motion direction.
(A) Delay epoch, orientation and motion direction trials combined.
(B) Delay epoch, orientation trials.
(C) Delay epoch, motion direction trials (opposite direction conditions sharing the same orientation axis combined).
(D) Stimulus encoding epoch, motion direction trials (separately for each of the 6 direction conditions).
(E) Delay epoch, motion direction trials (separately for each of the 6 direction conditions).
For all figures, the size of each map is from -20° to 20° of visual angle (dva), and the stimulus size is shown for reference in black circles. For (D-E) each of the 6 motion direction schematics on the top correspond to each of the 6 maps for a given ROI.

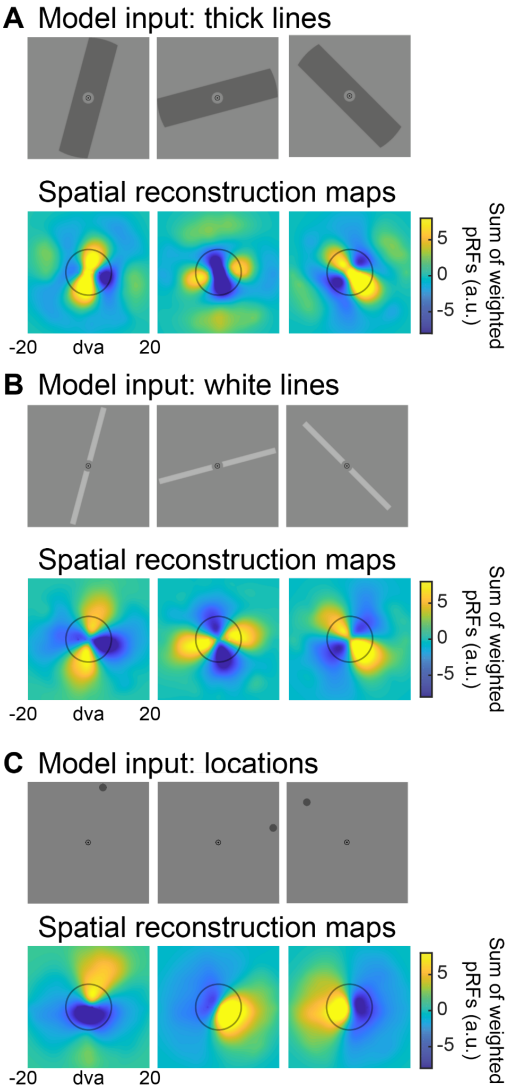

Testing other hypothetical working memory representations with the image-computable model of V1, related to Figure 4. Various image types were fed into the image-computable model of V1 to test other possible working memory formats that could have resulted in the spatial line format parallel to the remembered grating orientation and dot motion direction.
(A) Manipulating the width of the line images led to the same spatial line format as observed in the bottom panel of Figure 4B.
(B) Manipulating the color of the line images resulted in the same spatial line format as observed in the bottom panel of Figure 4B.
(C) The spatial line formats in the bottom panel of Figure 4B did not result from visualizing the location in space forming an angle that matches the remembered feature.